정다각형 단면을 갖는 일정체적 변단면 기둥의 정확탄성곡선

Elastica of Tapered Columns of Regular Polygon Cross-Section with Constant Volume

이 병 구[1] · 오 상 진[2] · 모 정 만[2]
By LEE, Byoung Koo OH, Sang Jin and MO, Jeong Man

ABSTRACT : 본 논문에서는 단순지지된 일정체적의 정다각형 단면을 갖는 변단면 기둥의 정확탄성곡선(elastica)을 산출할 수 있는 수치해석법을 개발하였다. 정확탄성곡선의 미분방정식은 Bernoulli-Euler 보 이론으로 유도하였고, 미분방정식의 수치적분은 Runge-Kutta method를 이용하였다. 미분방정식의 고유치인 지점의 단면회전각은 Regula-Falsi method를 이용하여 계산하였다. 변단면의 단면 깊이의 변화식으로는 직선식, 포물선식 및 정현식의 3가지 함수식을 채택하였다. 또한 유도된 미분방정식을 이용하여 대상기둥의 좌굴하중을 산출하고 이로부터 최강기둥의 단면비와 좌굴하중을 결정하였다.

1. Introduction

The first studies of the elastica were published in 1774 by Euler[1]. A survey of the classical literature on this subject was published in 1971 by Schmidt and Da Deppo[2]. Present-day applications of elastica included statics and dynamics problems were discussed by B.K. Lee et al.[3] and Wilson et al.[4], respectively. Other works related to the present studies, especially those involving uniform beams are in references[5-9].

Since columns are basic structural forms, these units has been widely used in the various engineering fields. In the column's problem, both the buckling loads and post-buckling behavior are very important to the structural design. It is clear that the column's behavior under loads depends on the cross-sectional shape, taper type and volume of the co-

1) Professor, Wonkwang University
2) Graduate Student, Wonkwang University

lumn[10,11]. Nowhere in the open literature were found solutions for the class of elastica problems considered herein: the elastica of non-uniform or tapered columns of regular polygon cross-section with constant volume, whose cross-sectional depths are varying in functional fashions. Therefor the main purpose of this paper is to investigate both the buckling loads and elastica of such columns.

In the analysis of elastica, one usually begins with classical Bernoulli-Euler beam theory, the non-linear differential equation that relates deflection to load. This beam theory is also used in the present analytical studies. The following assumptions are inherent in this theory: the column is linearly elastic, the neutral axis for bending is inextensible, and effects of Poisson's ratio and transverse shear deformation are negligible.

Historically, solutions of elastica have four forms : (1) closed-form solutions in terms of elliptic integrals ; (2) power series solutions : (3) numerical solutions : and (4) experimental solutions. The present study begins with an analysis involving theories and ends with numerical solutions using the Runge-Kutta and Regula-Falsi methods.

2. Object column

Shown in Figure 1(a) is the object column of length l and of constant volume V. Its cross-sectional shape is the regular polygon, whose cross-sectional depth depicted as h varies with the abscissa s. Thus the area and moment of inertia depicted as A and I, respectively, vary with s. Figure 1(b) shows the variation of depth h with s. As shown in this figure, the depths h at s=0 and l, and at s=$l/2$ are h_o and h_m, respectively. For defining geometry of column, a non-dimensional system parameter or section ratio n is introduced as follows.

$$n = h_m / h_o \tag{1}$$

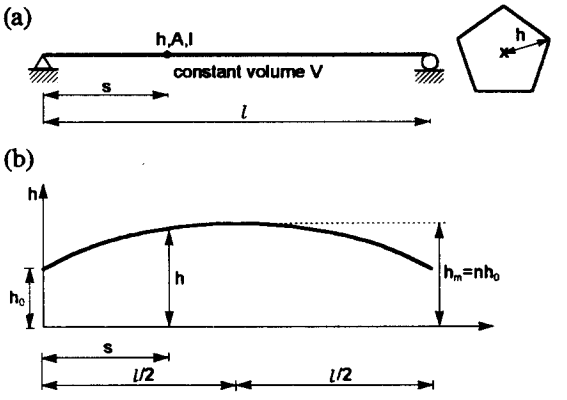

Figure 1. Column with constant volume and its variation of cross-sectional depth

The area A and moment of inertia I of the regular polygon cross-section with integer number m of sides of polygon and cross-sectional depth h are given by

$$A = c_1 h^2 \tag{2}$$

$$I = c_2 h^4 \tag{3}$$

where,

$$c_1 = m \sin(\pi/m)\cos(\pi/m) \tag{4.1}$$

$$c_2 = m \sin(\pi/m)\cos^3(\pi/m)\,[1+\tan^2(\pi/m)/3]/4 \tag{4.2}$$

in which it is clear that values of c_1 and c_2 with infinite number m, namely circular cross-section, are converged to π and $\pi/4$, respectively. Also, it is noted that every centeroidal

axis of regular polygon cross-section is the principal axis and has same moment of inertia given in equation (3).

Now, consider the functional equations of variable depth h. In this study, the linear, parabolic and sinusoidal tapers are chosen as the variable h of tapered columns. First, the equation h of linear taper through three points of $(0, h_o)$, $(l/2, nh_o)$ and (l, h_o) in rectangular co-ordinates (s, h) are obtained as follows.

$$h = h_o[2c_3(s/l)+1],\ 0 \le s \le l/2 \text{ and}$$
$$h = h_o[-2c_3(s/l)+2c_3+1],\ l/2 \le s \le l \quad (5)$$

where,

$$c_3 = n-1 \quad (6)$$

The column's volume V can now be calculated by using equations (2) and (5):

$$V = \int_0^l A\,ds = c_1 h_o^2 l c_4 \quad (7)$$

where,

$$c_4 = V/(c_1 h_o^2 l) = (n^2+n+1)/3 \quad (8)$$

in which c_4 is defined as a ratio of constant volume V to volume of uniform column of regular polygon cross-section with depth h_o, $c_1 h_o^2 l$.

Second, the equation h of parabolic taper is given by

$$h = h_o[-4c_3(s/l)^2+4c_3(s/l)+1],\ 0 \le s \le l \quad (9)$$

The column's volume V can be obtained by equation (7) with the following c_4.

$$c_4 = (8n^2+4n+3)/15 \quad (10)$$

Finally, the equation h and c_4 value of sinusoidal taper are, respectively,

$$h = h_o[c_3 \sin(\pi s/l)+1],\ 0 \le s \le l \quad (11)$$
$$c_4 = (n-1)^2/2+4(n-1)/\pi+1 \quad (12)$$

In equations (9) and (11), c_3 is same as equation (6).

3. Mathematical model

The symbols and loading for the buckled shape of object column defined in above section are depicted in Figure 2. The column is supported by the hinged and movable ends. The column subjected to an axial load P less than the buckling load B is perfectly straight. But when the P exceeds the B, the column is buckled. The dashed line and the solid curve are the neutral axes of the unbuckled and buckled column, respectively. The elastica of buckled column is defined by the (x, y) co-ordinate system whose origin is at hinged end. At a reference material point (x, y), the column's arc length is s, and the variable area and moment of inertia taken with respect to s are A and I, respectively. And the rotation of cross-section and bending moment are depicted as θ and M, respectively. It is noted that the axis length of buckled column maintains its length l due to inextensibility of column, and therefore the s value at movable end is l. The rotation at hinged end(s=0) and the horizontal displacement at movable end (s=l) are α and Δ, respectively. It is assumed that Bernoulli-Euler theory governs the

buckled column behavior under load, for which the differential equations for the elastica[6] is

$$d\theta/ds = -Py/EI,\ 0 \le s \le l \quad (13)$$

$$dx/ds = \cos\theta,\ 0 \le s \le l \quad (14)$$

$$dy/ds = \sin\theta,\ 0 \le s \le l \quad (15)$$

where E is Young's modulus and the term of Py in equation (13) is the bending moment M at the material point (x, y).

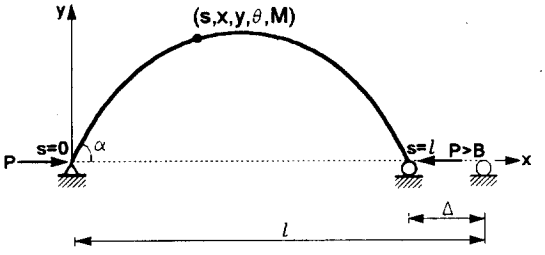

Figure 2. Variables of elastica of buckled column

Since the horizontal and vertical displacements at hinged end(s=0) are not allowed, the following boundary conditions are obtained:

$$x = 0 \text{ at } s = 0 \quad (16)$$

$$y = 0 \text{ at } s = 0 \quad (17)$$

Since the vertical displacement at movable end(s=l) is not allowed, the boundary condition is

$$y = 0 \text{ at } s = l \quad (18)$$

To facilitate the numerical studies and to obtain the most general results for this class of problem, the axial load, the geometric parameters, and the governing differential equations with their boundary conditions are cast in the following non-dimensional forms. The first is the load parameter,

$$p = P\,l^2/(\pi^2 EI_e) \quad (19)$$

where I_e is the moment of inertia of circular cross-section of uniform column whose volume is V, defined as

$$I_e = (V/2l)^2/\pi \quad (20)$$

The arc length s and coordinates (x, y) are normalized by the column length l, or

$$\lambda = s/l \quad (21)$$

$$\xi = x/l \quad (22)$$

$$\eta = y/l \quad (23)$$

The displacement Δ of movable end is also normalized by l, or

$$\delta = \Delta/l \quad (24)$$

When equation (3) combined with equation (5) or equation (9) or equation (11), and equations (19)-(23) are used, the non-dimensional form of equation (13) becomes

$$d\theta/d\lambda = -\pi c_1^2 c_4^2 p/(4c_2 i),\ 0 \le \lambda \le 1 \quad (25.1)$$

where,

for linear taper : $i = 2c_3\lambda + 1,\ 0 \le \lambda \le 0.5$ and

$$i = -2c_3\lambda + 2c_3 + 1,\ 0.5 \le \lambda \le 1 \quad (25.2)$$

for parabolic taper : $i = -4c_3\lambda^2 + 4c_3\lambda + 1,$

$$0 \le \lambda \le 1 \quad (25.3)$$

for sinusoidal taper : $i = c_3\sin(\pi\lambda) + 1,$

$$0 \le \lambda \le 1 \quad (25.4)$$

Further, with equations (21)-(23), equations (14) and (15) become

$$d\xi/d\lambda = \cos\theta,\ 0 \le \lambda \le 1 \quad (26)$$

$$d\eta/d\lambda = \sin\theta,\ 0 \le \lambda \le 1 \quad (27)$$

The non-dimensional forms for boundary conditions of equations (16)-(18) are obtained by equations (21)-(23):

$$\xi = 0 \text{ at } \lambda = 0 \tag{28}$$

$$\eta = 0 \text{ at } \lambda = 0 \tag{29}$$

$$\eta = 0 \text{ at } \lambda = 1 \tag{30}$$

4. Numerical methods

Based on above analysis, an algorithm was developed to solve differential equations (25.1), (26) and (27). The Runge-Kutta and Regula-Falsi methods[12] were used to integrate differential equations and to determine the initial rotation of cross-section for a given geometry of column. This algorithm is summarized as follows.

(1) Specify taper type(linear/parabolic/sinusoidal) and geometry (m, n, p) and then calculate c_1-c_4. It is recall that m is the integer number of sides of regular polygon cross-section.

(2) Assume a trial value α_t in which first trial value is zero.

(3) Integrate equations (25.1), (26) and (27) with equations (28) and (29) in the range from λ=0 to 1 using the Runge-Kutta method. The results give trial solutions for $\theta=\theta(\lambda)$, $\xi=\xi(\lambda)$ and $\eta=\eta(\lambda)$.

(4) Set $D=\eta(1)$. If the value of α_t assumed in step 2 is the characteristic value of the elastica, then D must be zero due to equation (30). The first criterion for convergence of the solutions is $|D| \leq 1\times 10^{-10}$

(5) If the value of D does not satisfy the first convergence criterion, then increment the previous value of α_t.

(6) Repeat steps (3)-(5) and note the sign of D in each iteration. If D changes sign between two consecutive values α_1 and α_2 of α_t, then the characteristic value α lies between α_1 and α_2.

(7) Compute advanced value of α_t based on its two previous values using the Regula-Falsi method. The second criterion for convergence of solutions is $|(\alpha_2-\alpha_1)/\alpha_2| \leq 1\times 10^{-5}$.

(8) Terminate the calculations when two convergency criteria are met. And print final solutions to the elastica, $\theta=\theta(\lambda)$, $\xi=\xi(\lambda)$ and $\eta=\eta(\lambda)$, and then compute the displacement $\delta=1-\xi(1)$. If there is no solution, which means that D does not change sign till the trial value of α_t reaches at π, the specified p is less than b and the column is still straight. Here, b is the buckling load parameter defined as

$$b=Bl^2/(\pi^2 EI_e) \tag{31}$$

Also, the buckling load parameters b were calculated in a straightforward way using the differential equations. Just after the column is buckled, all values of column behavior including α are close to zero. In this study, the buckling load parameter b is approximately equivalent to the load parameter p whose rotation α is 1×10^{-10}, i.e. nearly zero but not zero. Specify column taper, m, n, of course not p and set $\theta=1\times 10^{-10}$ at λ=0 in equations (26) and (27). And assume the trial value p instead of α_t in step 2. Remaining numerical

procedures are same as above procedure, and of course the characteristic value of equation (25.1) is p which is now an approximate buckling load parameter.

Based on these algorithms, two FORTRAN computer programs were written to solve the elastica and buckling loads, respectively. All computations were carried on a personal computer with graphics support. For all of the numerical results presented herein, a step size of 1/50 in the Runge-Kutta method was found to give convergence for α and b to within three significant figures. The numerical results are now discussed in next section.

5. Numerical results and discussion

Shown in Figure 3 are the equilibrium paths of linear taper with m=3, 4 and c(circular cross-section) for n=1.5, which represent the deflections(α/π, δ and $\eta_{\lambda=0.5}$) versus p curves after buckling. Just after buckling of the column, as the integer number m increases from m=3 to m=4 to m=c, all deflections increase, other parameters remaining constant. But it is true that $\eta_{\lambda=0.5}$ is decreased when p exceeds some characteristic value. Also, it is seen that the p values marked □ are the buckling load parameters b of corresponding columns. For example, it is clear that the b of m=3 is 1.484.

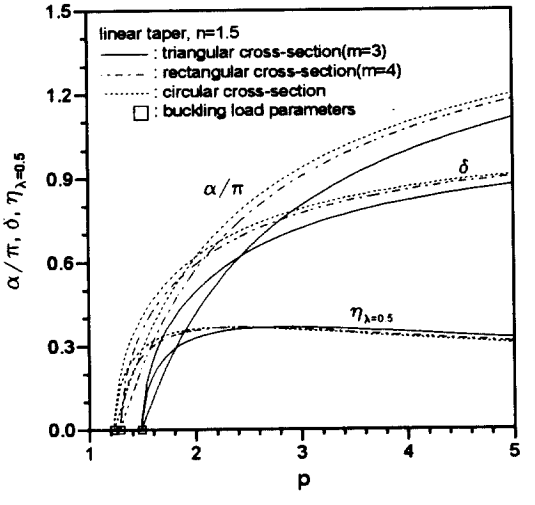

Figure 3. Equilibrium path of linear taper with n=1.5 by side number m

Shown in Figure 4 are the equilibrium paths of parabolic, sinusoidal and linear tapers for m=3 and n=2.5. Just after buckling, as the taper type is increased from parabolic to sinusoidal to linear taper, all deflections increase, other parameters remaining constant. But when p exceeds some characteristic value, the fact is reversed. Also, the buckling load parameters are marked by □ on the p axis.

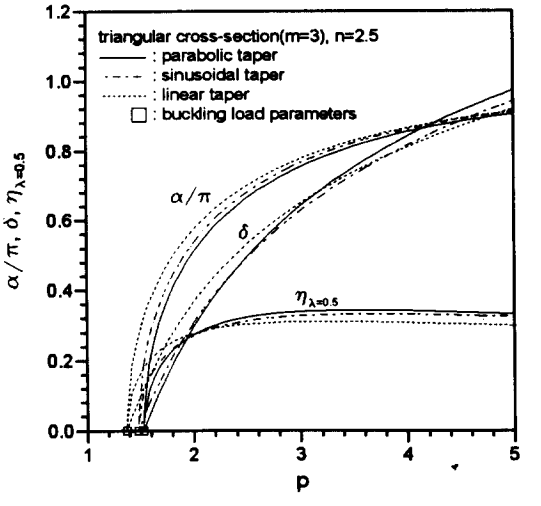

Figure 4. Equilibrium path of columns with m=3 and n=2.5 by taper type

Figure 5 are the elastica of linear taper with m=3, 4, 5 and c for n=1.5 and p=1.8. From this figure, it is seen that as the m value

increases from 3 to c, the horizontal and vertical deflections increase.

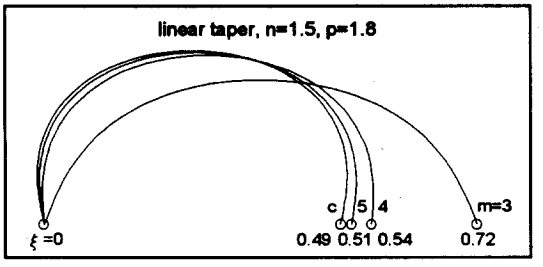

Figure 5. Elastica of linear taper with n=1.5 and p=1.8 by side number m

Shown in Figure 6, 7, 8 are the b versus n curves of columns with m=3, 4, 5 and c for linear, parabolic and sinusoidal taper, respectively. Each curve reaches a peak which is marked by □. At these peak points, the columns show the biggest b values which are the buckling load parameters of the strongest columns. It is found that all strongest columns are arose at the same value n if the taper type is same. And all b values of strongest columns decrease, as the m value increases from 3 to c. The values of b and n of all strongest columns are summarized in Table 1. From this table, it is noted that all b values of strongest columns are biggest at m=3(triangular cross-section) and smallest at m=c(circular cross-section), and the ratios of m=3 to m=c are same, i.e. 1.210, regardless of taper types.

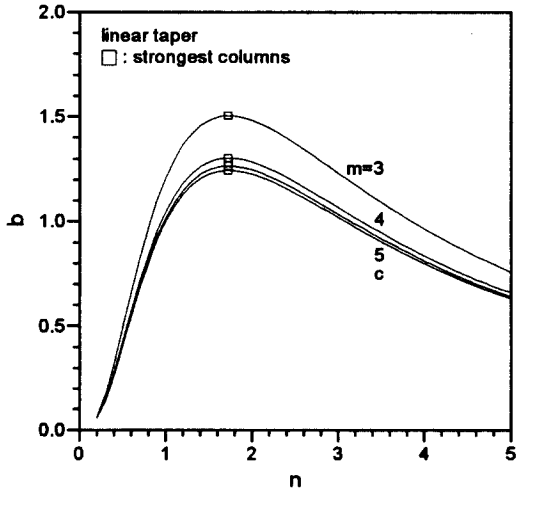

Figure 6. b vs. n curves of linear taper by side number m

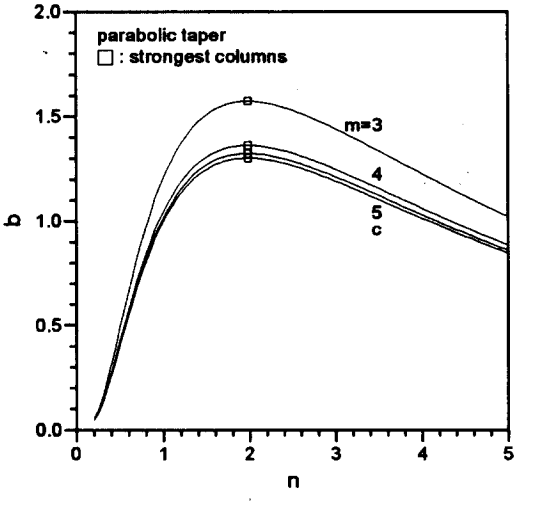

Figure 7. b vs. n curves of parabolic taper by side number m

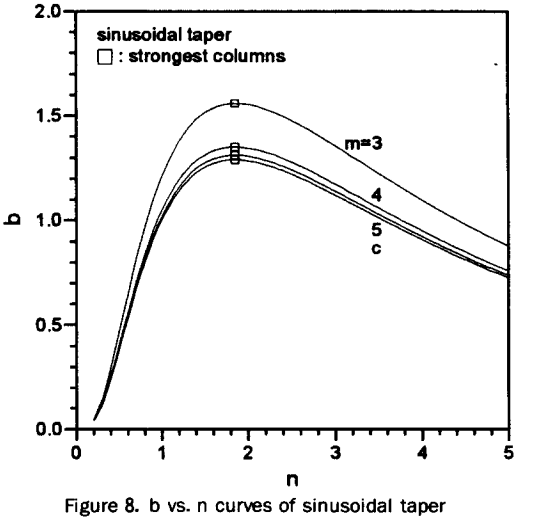

Figure 8. b vs. n curves of sinusoidal taper by side number m

Table 1. Values of n and b of strongest columns by taper type

taper type	m	n	b	ratio**
linear taper	3	1.72	1.505	1.210
	4	1.72	1.303	1.047
	5	1.72	1.265	1.017
	c*	1.72	1.244	1.000
parabolic taper	3	1.98	1.574	1.210
	4	1.98	1.362	1.047
	5	1.98	1.323	1.017
	c	1.98	1.301	1.000
sinusoidal taper	3	1.85	1.559	1.210
	4	1.85	1.350	1.047
	5	1.85	1.311	1.017
	c	1.85	1.289	1.000

* circular cross section

** ratio of b of m=3, 4 and 5, respectively, to m=c

Shown in Figure 9 are the b versus n curves of parabolic, sinusoidal and linear tapers, respectively, for m=3, in which the strongest columns are marked by □. It is clear that the strongest column among the examined taper types is the parabolic tapered column as shown in this figure and Table 1. The effect of taper type on b is negligible before the n values corresponding to the strongest columns, but not negligible after these n values.

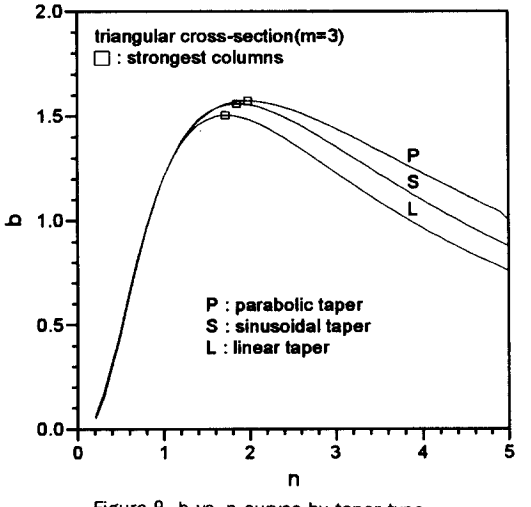

Figure 9. b vs. n curves by taper type

Shown in Figure 10 are the elastica of the strongest columns of m=3 and p=2 by taper type. It is clear that the horizontal and vertical deflections increase, as the taper type increases from parabolic to sinusoidal to linear taper, other parameters remaining constant.

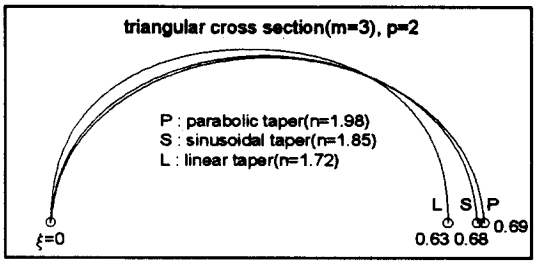

Figure 10. Elastica of strongest columns with m=3 and p=2

6. Conclusions

The numerical methods developed herein for computing the elastica and buckling loads of tapered columns of regular polygon cross-section with constant volume were found to be efficient, and highly versatile. The differential equations governing the elastica of such column were derived and solved numerically. The linear, parabolic and sinusoidal tapers were chosen as the variable depth of cross-section. As the numerical results, the equilibrium paths and elastica were presented, and the buckling load parameter versus section ratio(b vs. n) curves were also reported. The strongest columns by taper type and side number of regular polygon cross section, respectively, were determined by reading the peak point of buckling load parameters and those

corresponding section ratios on b versus n curves.

References

1. L. Euler : Methodus Inveniendi Lineas Curvas Maxima Minimive Proprietate Gaudentes, Additamentum I, De Curvis Elasticis, Lausanne and Geneva, 1774.
2. R. Schmidt and D.A. Da Deppo : A Survey of Literature on Large Deflection of Nonshallow Arches, Bibliography of Finite Deflections of Straight and Curved Beams, Rings, and Shallow Arches, J. Ind. Math. Soc., Vol.21, No. 91, 1971.
3. B. K. Lee, J. F. Wilson and S. J. Oh : Elastica of Cantilevered Beams with Variable Cross-Section, Int. J. Non-Linear Mech., 28, No. 5, 1993, pp. 579-589.
4. J. F. Wilson and U. Mahajan : The Mechanics and Positioning of Highly Flexible Manipulator Limbs, J. Mech. Trans. Automat. Des. Vol. Ⅲ, 1989, pp. 232-236.
5. A. E. H. Love : A Treatise on the Mathematical Theory of Elasticity, Dover, New York, 1972.
6. S. P. Timoshenko and J. M. Gere : Theory of Elastic Stability, McGraw-Hill, 1961.
7. C. Rojahn, Large Deflections of Elastic Beam : Thesis for the Degree of Engineer, Standford University, 1968.
8. J. F. Wilson and J. M. Snyder : The Elastica with End-Load Flip-Over, J. Appl. Mech., Vol.55, 1988, pp. 845-848.
9. C. Y. Wang : Large Deflections of an Inclined Cantilever with an End Load, Int. J. Non-Linear Mech., Vol. 16, 1981, pp. 155-164.
10. J. M. Gere and S. P. Timoshenko : Mechanics of Materials, Brooks /Cole Engineering, 1984, p. 560.
11. R. T. Haftka, Z. Gürdal and M. P. Kamat : Elements of Structural Optimization, Kluwer Academic Publisher, 1990, pp. 40-52.
12. B. Carnahan, H. A. Luther and J. O. Wilkes : Applied Numerical Methods, John Wiley & Sons, Inc., 1969.